

# Wind Tunnel Tests on a Three-stage Out-phase Savonius Rotor

Tsutomu HAYASHI<sup>1</sup>, Yan LI<sup>2</sup>, Yutaka HARA<sup>3</sup> and Katsuya SUZUKI<sup>4</sup>

<sup>1</sup> Department of Applied Mathematics and Physics, Faculty of Engineering, Tottori University, 4-101 Koyama-cho Minami, Tottori, Japan; Tel: +81-857-31-6741, Fax: +81-857-31-5747, e-mail: hayashi@damp.tottori-u.ac.jp

<sup>2</sup> Graduate School of Engineering, Tottori University; e-mail: lee@svr01.damp.tottori-u.ac.jp

<sup>3</sup> Department of Applied Mathematics and Physics, Faculty of Engineering, Tottori University; Tel: +81-857-31-6758, e-mail: hara@damp.tottori-u.ac.jp

<sup>4</sup> Tottori University Visiting Professor; 2-74, Sumire-dai, Seto, Aichi, Japan; e-mail: kasuzuki2002jp@yahoo.co.jp

## Abstract

The torque characteristics of an ordinary Savonius rotor have two problems: the first one is the fairly large torque variation, and the second one is that there are some angular positions where the static torque is negative or very small. To improve such undesirable torque characteristics of Savonius rotor, a three-stage out-phase type Savonius rotor, which has three stages and buckets of which have 120-degree phase shift between the adjacent stages, was designed and made. Wind tunnel tests were carried out on this new type Savonius rotor and an ordinary one-stage rotor. The tests included the fluctuation measurements of the static and dynamic torques in one revolution, and the average torque measurements at different rotational speeds. The results can be summarized as follows: (1) the static torque coefficient of the three-stage rotor had a cycle of 60 degrees, which corresponded to the number of the buckets. The torque coefficient during one revolution is positive and its variation became very small to the extent of about 1/6 of the one-stage rotor. Therefore the starting performance has been greatly improved. (2) The maximum value of the power coefficient of the three-stage rotor was about 75% of that of the one-stage rotor due to the small aspect ratio of each stage of the three-stage rotor in our study. (3) The variation of the dynamic torque coefficient of the three-stage rotor was small than the one-stage rotor and had little dependency on tip speed ratio. By its smoothed variation of the dynamic characteristics, the durability of the three-stage rotor can be expected.

## 1. Introductions

Savonius rotor conceived by the Finnish Engineer S.J. Savonius<sup>(1)</sup> in 1931 is a kind of drag type vertical-axis wind turbine. A basic configuration of this rotor has a

“S-shaped” cross-section constructed by two semicircular buckets with a small overlap between them. And the principle of operation is based on the difference of drag between the convex and the concave parts of the buckets. By the advantages of simple design and low construction cost, Savonius rotor is mainly used for water pumping and wind power on a small scale. The large starting torque may allow Savonius rotor to find another use as a starter for the other type of wind turbines that have worse starting characteristic, such as Darrieus rotor, Gyro mill, etc. However, the Savonius rotor did not become popular for the purpose of electric power generation because of the low power efficiency in comparison with the lift type wind turbines. Recently, some generators suitable for small-scale wind turbines have been greatly developed, which have the characteristics of high torque in low rotational speed. Therefore, Savonius rotor might be used for electric power generation in quiet environment.

However, the torque characteristics of an ordinary Savonius rotor have two problems: the first one is the fairly large torque variation, which causes rotor's vibration and consequently decreases the rotor's durability. The second problem is that there are some angular positions where the static torque is negative or very small. This fact is an obstacle when Savonius rotor is used as a starter. In the past, many researchers focused on improving the torque characteristics of Savonius rotor. Shedahl conducted some wind tunnel tests on a three-bucket rotor<sup>(3)</sup>. Khan stacked an ordinary Savonius rotor on another rotor with 90-degree phase shift<sup>(4)</sup>. For both the three-bucket rotor and the two-stage rotor, the negative starting torque range was decreased and the torque variation became slightly smaller than the ordinary rotor. However, those torque variations were still large for the purpose of a starter device. A Savonius rotor with twisted blades was proposed<sup>(5)</sup>. The twisted rotor has good starting characteristics, but the cost

becomes high due to the complexity of blade shape. Some researchers focused on using auxiliary devices to improve the starting characteristics of Savonius rotor: Sivasegaram used an asymmetrical box with a funnel-shaped wind inlet<sup>(6)</sup>; Alexander used a flat shield and a circular shield<sup>(7)</sup>; Several static circular guide vanes were tried by Ogawa<sup>(8)</sup>.

In this study, a new type of Savonius rotor is proposed and it has been tested with the wind tunnel. The new type rotor was named by the authors to “Three-stage Out-phase Savonius Rotor” because it has three stages with 120-degree bucket phase shift between the adjacent stages. Stacking ordinary two-bucket type rotors with different phases is expected to give the torque averaging and the cost reduction. According to the authors’ knowledge, there are no reports on measurements about the torque variation in one revolution of such a three-stage out-phase Savonius rotor, which is called “three-stage rotor” simply hereafter. A number of wind tunnel tests were carried out on both the three-stage rotor and an ordinary one-stage rotor, for making comparisons under many conditions. The tests included the fluctuation measurements of the static and dynamic torques in one revolution, and the average torque measurements at different rotational speeds.

## 2. Nomenclature

$d$	=	Bucket diameter, m
$D$	=	Rotor diameter, m
$H$	=	Rotor height, m
$h$	=	Height of each stage of the three-stage rotor, m
$S$	=	Rotor overlap, m
$A_s$	=	Rotor swept area, m <sup>2</sup> ; $A_s = D \cdot H$
$A_T$	=	Wind tunnel outlet area, m <sup>2</sup>
$\beta$	=	Blockage ratio; $\beta = \frac{A_s}{A_T}$
$OL$	=	Rotor overlap ratio; $OL = \frac{S}{D}$
$AR$	=	Aspect ratio of test rotors; $AR = \frac{H}{d}$
$Ar$	=	Aspect ratio of each stage of the three-stage rotor; $Ar = \frac{h}{d}$
$U$	=	Wind velocity, m/s
$\rho$	=	Density of air, kg/m <sup>3</sup>

$\nu$	=	Kinematic viscosity, m <sup>2</sup> /s
$Re$	=	Reynolds number; $Re = \frac{UD}{\nu}$
$n$	=	Rotor revolution, rpm
$\omega$	=	Rotor angular speed, rad/s;
$\alpha$	=	Bucket rotation angel, degree
$\lambda$	=	Tip speed ratio; $\lambda = \frac{\omega D}{2U}$
$T$	=	Torque, N·m
$T_s$	=	Static torque, N·m
$P$	=	Power, W
$C_t$	=	Torque coefficient;
		$C_t = \frac{T}{\frac{1}{4} \rho A_s D U^2}$
$C_{ts}$	=	Static torque coefficient;
		$C_{ts} = \frac{T_s}{\frac{1}{4} \rho A_s D U^2}$
$C_p$	=	Power coefficient;
		$C_p = \frac{P}{\frac{1}{2} \rho A_s U^3}$

## 3. Experimental Detail

### 3.1 Test Models

Figure 1 shows the geometry of the three-stage rotor and the one-stage rotor, and the main sizes of the two rotors are listed in Table 1. The performance measurements were carried out in an open-circuit wind tunnel with an outlet section of  $1.5 \times 1.5$  m<sup>2</sup>, which generates wind speed up to 25m/s. The previous studies<sup>(3), (7)</sup> showed that large blockage ratio affected the rotor performance. Thus, the rotors used in this study have relatively small swept area of  $A_s=0.076$  m<sup>2</sup>, which give the wind tunnel blockage ratio of 3.5%. According to Ushiyama, a rotor with large aspect ratio gets better power efficiency<sup>(9)</sup>. However, considering the importance of small blockage ratio and convenience of measurement, aspect ratio  $AR = 1.25$  was selected for both types of the test rotors. Therefore, the aspect ratio for each stage of the three-stage rotor is  $Ar = 0.4$ . The overlap ratio of the test rotors was decided as  $OL=0.2$  according to the other researchers’ studies, in which the proper overlap ratios were found between 0.15 and 0.25<sup>(3), (9)</sup>.

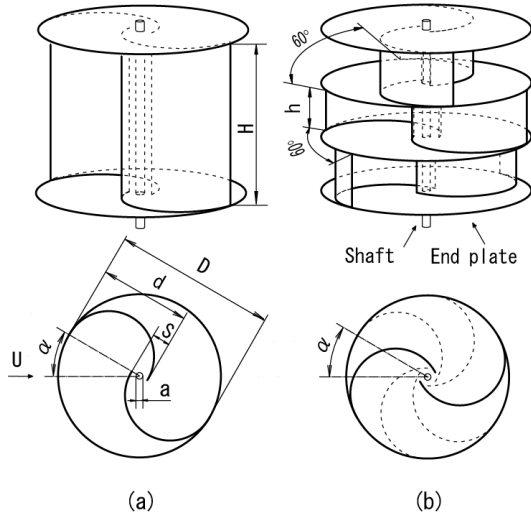


Figure 1. Geometry of the test rotors (a) the one-stage rotor, (b) the three-stage rotor

Table 1: Main sizes of the test rotors

D	0.33m	d	0.184m
H	0.23m	h	0.074m
S	0.066m	a	0.015m

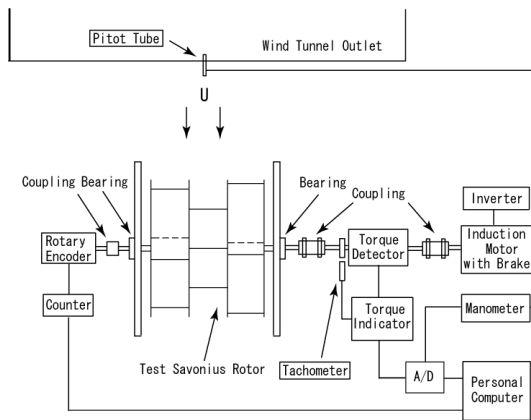


Figure 2. The schematic diagram of the experimental system

### 3.2 Experimental methodology

Figure 2 shows the schematic diagram of our experimental system. Although Savonius rotor is a kind of vertical-axis wind turbine, considering the convenience of measurements, the rotor axis was set up horizontally. The test rotor was placed 2m downstream from the wind tunnel outlet at the height of the center of the outlet cross section. The rotor torque was measured by a digital torque detector (ONO SOKKI, SS-010), which was located between the

rotor and an induction motor equipped with a brake (MITSUBISHI ELECTRIC, ZKB-2.5HBN). The sampling time of the data acquisition is 1ms. The revolution of the induction motor was controlled by an inverter, and the rotational speed was measured by a digital tachometer. A rotary encoder (ONO SOKKI, RP-432Z) was used to measure the rotation angle  $\alpha$  of the rotor shaft. Wind speed was measured by a Pitot tube.

When the static characteristics were measured, the rotor shaft was fixed by the brake of induction motor. The static torque was measured at a fixed bucket rotation angle and was averaged for ten seconds under a steady wind speed. This static measurements were repeated every 5-degree of bucket rotation angle  $\alpha$  for a specific condition. Wind speeds for the static measurements of the rotors were 6, 9 and 12 m/s, which correspond to the Reynolds numbers of  $1.4 \times 10^5$ ,  $2.1 \times 10^5$ , and  $2.8 \times 10^5$ , respectively.

In the rotor performance measurements, a rotor was operated with a constant rotational speed under a steady wind speed ( $U=6, 9, 12, 15$  and  $18$ m/s). The torque during rotation was measured for ten seconds and was averaged. The whole torque characteristics were obtained by changing the conditions of rotational speed and wind speed. The dynamic torque variation in one revolution under 12m/s was obtained by the simultaneous measurements of torque and rotation angle using the sampling time of 0.5ms. The data was ensemble-averaged for about 100 revolutions.

## 4. Results and Discussions

### 4.1 Static torque characteristics

Figure 3 shows the averaged static torque variations in one revolution of the test rotors at different wind speeds.

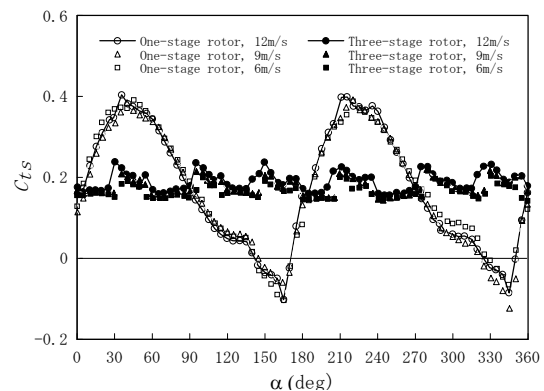


Figure 3. Static torque coefficient  $C_{ts}$  in one revolution

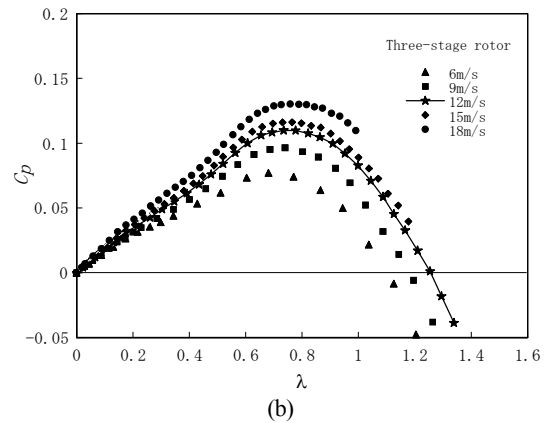
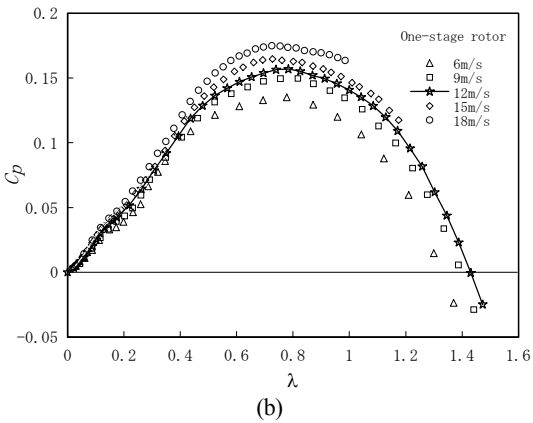
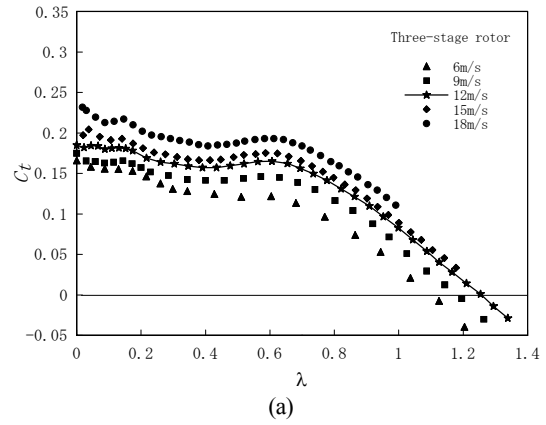
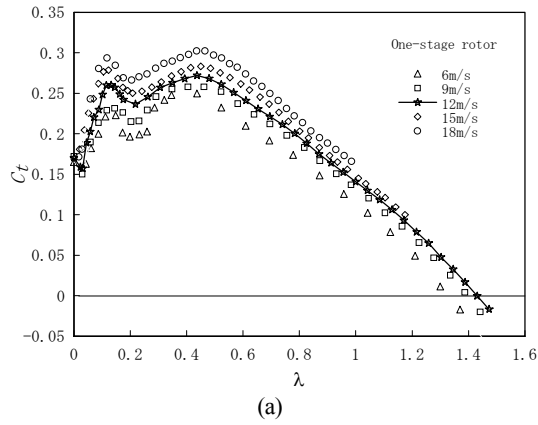


Figure 4. The torque and power characteristics of the one-stage rotor as a function of tip speed ratio: (a) torque coefficient, (b) power coefficient

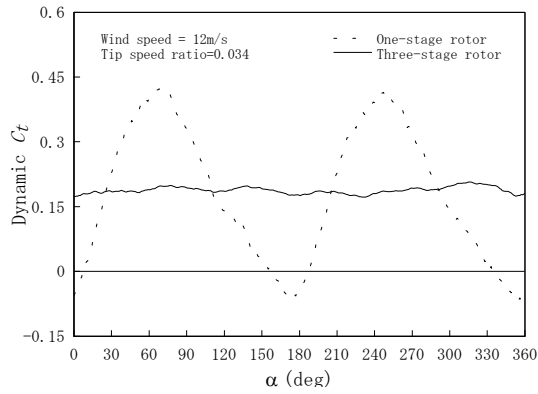
Figure 5. The torque and power characteristics of the three-stage rotor as a function of tip speed ratio: (a) torque coefficient, (b) power coefficient

It is found that the wind speed, that is, the Reynolds number  $R_e$ , has little effect on the static torque coefficients  $C_{ts}$  for both types of the test rotors in our experimental conditions ( $U=6, 9, 12\text{m/s}$ ). For distinct comparisons, the data under  $12\text{m/s}$  are linked by lines. The  $C_{ts}$  of the one-stage rotor has a cycle of  $180^\circ$  and the variation of  $C_{ts}$  is very large. Note that the value of  $C_{ts}$  becomes negative in the ranges of the angle  $\alpha=140^\circ \sim 170^\circ$  and  $320^\circ \sim 350^\circ$ . The maximum values of the  $C_{ts}$  appear near the angles of  $40^\circ$  and  $210^\circ$ . It also should be noted that there are two small bumps in the  $C_{ts}$  variations at the angles around  $135^\circ$  and  $315^\circ$ . The bumps are attributed to the overlap<sup>(9)</sup>. On the other hand, the  $C_{ts}$  of the three-stage rotor has a cycle of  $60^\circ$ , which corresponds to the number of the buckets. The peak-to-peak value of the static torque coefficient becomes small to the extent of about  $1/6$  of that of the one-stage rotor. In another word, the static torque of the three-stage rotor is averaged and kept almost

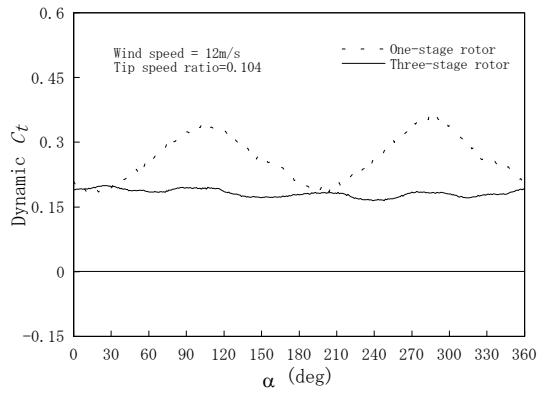
constant. The starting characteristics are greatly improved. Additionally, a bump is observed in each cycle of the  $C_{ts}$  beside the main torque peak. The bump may be also attributed to the overlap of each stage of the three-stage rotor by the similarity to the one-stage rotor.

#### 4.2 Performance of test rotors

Figures 4 and 5 are the torque coefficient  $C_t$  and the power coefficient  $C_p$  of the test rotors. The horizontal axis in each figure is the tip speed ratio  $\lambda$  and the data were measured under the conditions of  $U=6, 9, 12, 15$  and  $18\text{m/s}$ , which correspond to Reynolds number of  $R_e = 1.4 \times 10^5, 2.1 \times 10^5, 2.8 \times 10^5, 3.5 \times 10^5, \text{ and } 4.2 \times 10^5$ , respectively. For distinct comparisons, only the data under  $12\text{m/s}$  are linked by lines. Unlike the static characteristics shown in Fig. 3, the characteristics during rotation depend on wind speed. The results in Figs.4 and Figs.5 show the degradation of rotor performance due to the decrease of  $R_e$ . Note that the maximum value of  $C_t$  or  $C_p$  of the three-stage



(a)



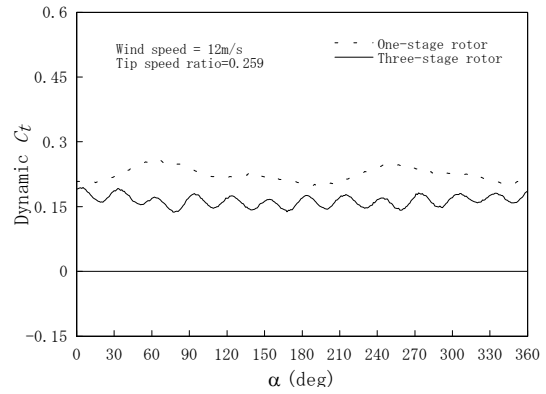
(b)

Figure 6. Dynamic torque coefficients of the two test rotors at the tip speed of (a)  $\lambda=0.034$ , (b)  $\lambda=0.104$

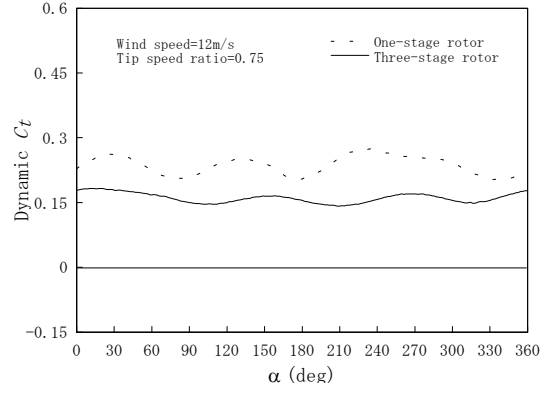
rotor at each wind speed is about 75% of that of the one-stage rotor. The much inferiority of the three-stage rotor is mainly caused by small aspect ratio of each stage as described before. As shown in the other study<sup>(9)</sup>, the difference of power coefficients between the rotors with three-time difference of aspect ratio is about 20~30%. If the aspect ratio of each stage of the three-stage rotor is enlarged, the performance can be expected to increase up to the same level of the one-stage rotor.

#### 4.3 Dynamic torque variation in one revolution

Figures 6 and 7 show the dynamic torque coefficients  $C_t$ , which were ensemble-averaged with the data for about 100 revolutions at some certain tip speed ratios ( $\lambda=0.034, 0.104, 0.259$  and  $0.75$ ). The wind speed for the experiments is 12 m/s and the origin of the bucket rotation angle  $\alpha$  is upwind direction. The behavior of dynamic torque of the two test rotors at  $\lambda=0.034$  is almost the same as the static torque behavior shown in Fig.3. The  $C_t$  of the one-stage rotor has two main large torque peaks in one revolution. And it can also be found that the negative value



(a)



(b)

Figure 7. Dynamic torque coefficients of the two test rotors at the tip speed of (a)  $\lambda=0.259$ , (b)  $\lambda=0.75$

still remains in two  $\alpha$  ranges during rotation at the low tip speed ratio. On the other hand, the  $C_t$  of the three-stage rotor has six torque peaks in one revolution, which corresponds to the number of buckets with different phases. However, with the increasing of tip speed ratio, the variation and the number of the torque peaks of both the one-stage rotor and the three-stage rotor varied. Although the reasons for this are still unclear for us, it could be considered that the effect of the overlap might be a main factor. Overlap might take different roles on the characteristics of the two type rotors at different tip speed ratios.

Figure 8 shows the peak-to-peak value of  $C_t$  for each rotor as a function of  $\lambda$  under  $U=12\text{m/s}$ . The peak-to-peak value of  $C_t$  of the one-stage rotor is large at low tip speed ratios, and it decreases with increasing  $\lambda$  between 0 and 0.5. Then the peak-to-peak value tends to increase gradually again for the larger  $\lambda$  ( $> 0.5$ ). On the other hand, the peak-to-peak value of  $C_t$  of the three-stage rotor is relatively smaller than the one-stage rotor and has

little dependency on  $\lambda$ . Therefore, the variation of the dynamic torque for the three-stage rotor has become smooth with independent of rotation speed. Consequently the increase of durability of the three-stage rotor can be expected.

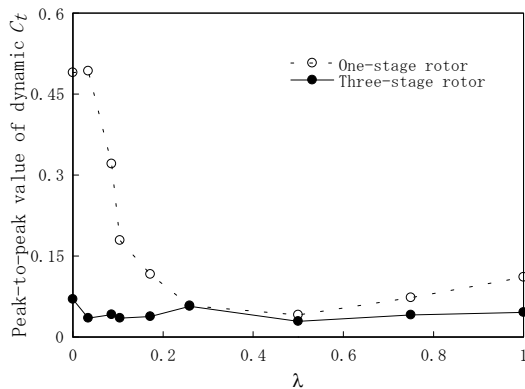


Figure 8. Peak-to-peak value of dynamic torque coefficient in one revolution of the two test rotors under  $U=12\text{m/s}$

### 5. Conclusions

A three-stage out-phase rotor was made in order to improve the torque characteristics of Savonius rotor. The characteristics of the three-stage out-phase Savonius rotor and an ordinary one-stage rotor were compared based on the results of the wind tunnel tests. The results can be summarized as follows:

(1) The variation of the static torque of the one-stage rotor was very large and had a cycle of 180 degrees. And the static torque took negative value in some certain ranges of the rotational angle. The static torque of the three-stage rotor had a cycle of 60 degrees, which corresponded to the number of the buckets. The static torque in one revolution was positive and the variation became very small to the extent of about 1/6 of the one-stage rotor. The bumps were observed in each cycle of the static torque of two test rotors and they were attributed to the overlap.

(2) The rotor performance during rotation had dependency on wind speed. The maximum value of the power coefficient of the three-stage rotor was 75% of the one-stage rotor. However, this inferiority of the three-stage rotor could be improved by enlarging the aspect ratio of each stage of the three-stage rotor.

(3) The peak-to-peak value of the dynamic torque coefficient of the three-stage rotor was small and had little dependency on tip speed ratio, whereas the peak-to-peak

value of the one-stage rotor dependent on the rotation speed and had large value at low tip speed ratio. Owing to the smoothed variation of the dynamic characteristics, the durability of the three-stage rotor can be expected.

### Acknowledgements

This study was carried out as a part of the "Program for Arid Land Science", which is one of the "21st Century COE Program" of the Ministry of Education, Culture, Sports, Science and Technology in Japan. We would like to express thanks to their supports.

### Reference

1. Savonius, S.J., Mechanical Engineering, The S-rotor and its application. Vol. 53, No. 5, pp. 333-338, 1931.
2. Wu, W., Ramsden, V.S., Crawford, T., Hill, G. A low-speed, high-torque, direct-drive permanent magnet generator for wind turbines. The 2000 IEEE Industry Application Conference, Vol. 1, pp. 147-154.
3. Shedahl, R.E., Blackwell, B.F. and Feltz, L.V. Wind tunnel performance data for two- and three-bucket Savonius rotor. AIAA Journal of Energy, Vol. 2, No. 3, pp. 160-164, 1978.
4. Khan, M. H. Model and prototype performance characteristics of Savonius rotor windmill. Wind Engineering, Vol.2, No. 2, pp. 75-85, 1978.
5. Grinspan, A. S., Suresh Kumar, P., Saha U. K., and Mahanta, P. Performance of Savonius wind turbine rotor with twisted bamboo blades. Proceedings of 19th Canadian congress of applied mechanics, Calgary, Alberta, Canada, Vol. 2, pp. 412 - 413, 2003.
6. Sivasegaram, S. Design parameters affecting the performance of resistance-type vertical-shaft wind rotors - an experimental investigation. Wind Engineering, Vol.1, No. 3, pp. 207-217, 1977.
7. Alexander, A.J. and Holownia, B.P. Wind tunnel tests on a Savonius rotor. Journal of industrial Aerodynamics, Vol.3, pp. 343-351, 1978.
8. Ogawa, T., Tahara, K., and Suzuki, N. Wind tunnel performance data of the Savonius rotor with circular guide vanes. Bulletin of JSME, (in Japanese) Vol. 29, No. 253, pp. 2109-2114, 1986.
9. Ushiyama, I., Nagai, H. and Shinoda, J. Experimentally determining the optimum design configuration for Savonius rotors. Trans. of JSME, Vol. 52, No. 480, pp. 2973-2982, 1986.